Assessing the Impact of Common Errors in Spherical Near-Field Measurements on the Evaluation of AUT Performance at Finite Distances

F. Saccardi *AMTA Fellow*, A. Giacomini, *Senior AMTA*, J. Singh, L. Foged, *AMTA Fellow*
Microwave Vision Italy SRL,
Via dei Castelli Romani 59, 00071, Pomezia, Italy
francesco.saccardi@mvg-world.com

S. Anwar, *AMTA Member*
MVG Industries, 13 rue du Zéphyr
Villejust, France
shoaib.anwar @mvg-world.com

***Abstract*—The objective of this paper is to provide some guidelines about the measurement uncertainty of Spherical Near Field (SNF) ranges when they are used to derive near field figure of merits instead of more conventional far field-based metrics.**

One of the main advantages of the SNF ranges is their flexibility. Indeed, from the NF scanning, the spherical wave expansion is applied, and it can be used as a powerful, accurate and efficient propagation tool, able to evaluate figures of merits at (almost) any distance from the device under test. This feature is particularly useful in the testing of modern antenna systems intended to operate in specific regions of space instead of conventional far field scenarios. Examples are Plane Wave Generators (PWG) which create a uniform field distribution in the proximity of the device, or more generic field synthesizer devices.

Despite the flexibility of SNF systems, the evaluation of their uncertainty budgets is normally limited to far field-based metrics. Understanding under which conditions and in which measurement scenarios such uncertainty budgets are applicable to more generic near field metrics is the main topic addressed in this paper.

I. INTRODUCTION

Spherical Near-Field (SNF) testing techniques are considered among the most accurate and versatile methods for characterizing the radiating performance of Antennas or Devices Under Test (AUT/DUT) [1]-[3]. Unlike planar and cylindrical Near-Field (NF) techniques, SNF allows for the measurement of DUTs with varying directivities due to significantly reduced truncation of the scanning area [1].

Another significant advantage of SNF techniques is their ability to evaluate the radiating performance of a DUT at almost any distance [4]. Once the SNF acquisition at a given distance is completed, the Spherical Wave Expansion (SWE) is applied, and the Spherical Wave Coefficients (SWC) are computed [2]. In most cases, the Far-Field (FF) pattern is derived from the SWC, completing the conventional NF/FF transformation process [1]-[2]. The evaluation of the FF radiation pattern is the conventional approach because it allows for the computation of standard metrics (such as directivity, gain, and polarization [5]) defined at an ideal, infinite distance.

However, many modern applications are designed to operate at reduced distances, where free space losses are significantly lower. Examples include systems exploiting the so-called "NF focusing effect," which will be utilized in 6G telecom applications [6]. Similarly, modern measurement systems like Plane Wave Generators (PWG, Figure 1.) synthesize a plane wave condition in the NF of the device [7]-[8], often requiring accurate characterization of radiating performance at specific operational distances.

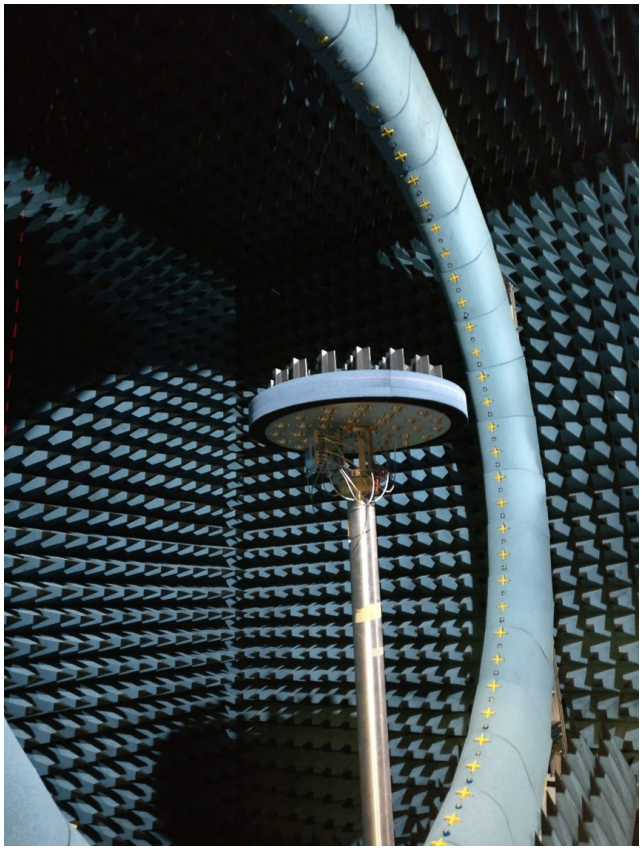

Figure 1. Example of PWG quiet zone testing in a spherical near field multiprobe system.

Understanding how measurement errors influence the measurement of specific NF figures of merit is of great interest, and to the best of the authors' knowledge, this has not been reported in the literature. This paper examines the effect of typical SNF measurement errors, such as residual chamber reflections, truncation errors and probe pattern effect considering different finite reconstruction distances.

Since uncertainty budgets of SNF ranges are usually evaluated assuming the conventional field transformation to FF, it is important to understand under which conditions such uncertainties can also be applied when arbitrary NF/NF transformations are performed.

The objective of the paper is hence to provide some preliminary guidelines regarding the validity of FF-based uncertainty budgets of SNF systems when such systems are exploited to evaluate specific NF metrics. For this purpose, different experimental examples will be taken into account.

These include the measurement of a dual-ridge horn antenna in which we will investigate how typical measurement error are propagated at significantly reduced reconstruction distances. This is particularly relevant when evaluating power densities at specific regulatory distances [9].

Moreover, an example of a PWG measured in a SNF system to test its QZ uniformity will be considered (see example shown in Figure 1). Gaining insights about the measurement uncertainty is of great interest, because such devices often have very stringent amplitude and phase QZ requirements, hence evaluating the measurement uncertainty is paramount to separate field variations due to the PWG itself from those coming from the measurement system.

II. Field Transformaton Process In SNF Measurements

In SNF measurements, the coupling signal between the AUT and the measuring probe(s) is acquired on a spherical surface of radius r (i.e. measurement sphere). From the measured data, the Spherical Wave Expansion (SWE) is applied considering the well—known transmission formula (TXF) [2],[10], reported in equation (1-2).

$$w(r,\chi,\theta,\varphi) = \sum_{\substack{smn \\ \mu}} Q_{smn}^{(4)} e^{jm\varphi} d_{\mu m}^{n}(\theta) e^{j\mu\chi} P_{s\mu n}^{(4)}(kr) \quad (1)$$

$$P_{s\mu n}^{(4)}(kr) = \sum_{\sigma\nu} C_{\sigma\mu\nu}^{sn(4)}(kr) R_{\sigma\mu\nu}^{p} \quad (2)$$

Such formula expresses the complex signal received by a probe (w) of known Spherical Wave Coefficients (SWC, $R_{\sigma\mu\nu}^{p}$) as a function of the probes coordinates (r,θ,φ) and orientation (χ) when an AUT described by its own SWC ($Q_{smn}^{(4)}$) transmits. The symbols $d_{\mu m}^{n}(\theta)$ and $C_{\sigma\mu\nu}^{sn(4)}(kA)$ are respectively rotation and translation operators that, together with the two complex exponentials ($e^{jm\varphi}$ and $e^{j\mu\chi}$), are used to describe the probe position/orientation in each measurement point. The quantity $P_{s\mu n}^{(4)}(kr)$ is called probe response constant and is traditionally written in a separated term because it only depends on the probe SWC, the measurement distance and the frequency.

The first SNF measurement processing step is the inversion of the TXF which allows the computation of the SWC of the AUT including, if needed, the compensation of the probe pattern effect [2], [11]. The SWC spectrum fully describes the radiation of the AUT everywhere in space outside the AUT minimum sphere (i.e. the smallest sphere centered in the origin of the coordinate system fully enclosing the AUT, [2]). The second processing step is the computation of the field at locations desired by the user.

In most of the applications, the AUT radiating performance at FF (infinite) distance are required. In such cases the TXF is applied as a forward operator, considering as input the AUT SWC previously computed, an ideal dipole located at infinite distance as probe and the wanted angular domain extension and resolution. This process is typically called NF/FF transformation and is performed in a very efficient manner (double-FFT both in the inversion of the TXF and in the FF computation [2]).

The field computation of the AUT at arbitrary finite-distance locations is required with other applications and it can easily be performed again using the TXF as forward operator (NF/NF transformation). The available SWC of AUT are again the main input, but the evaluation of the probe response constant, is performed at the wanted finite distance.

For example, by simply setting $r = r_0$, the field over a spherical surface of radius r_0 is efficiently computed (same complexity of computation as the NF/FF transformation). This feature is required for example to compute power densities at specific regulatory distances [9] or to compute the NF gain [10].

Other examples of reconstruction of arbitrary field distributions, are SNF measurements of devices like Plane Wave Generators (PWG) [7]-[8] or generic field synthesizers, which are intended to create a specific field distribution in a well-defined area (e.g. Quiet Zone, QZ, for PWGs systems). In such cases, the TXF is also used to compute the field in generic x,y,z cartesian positions (e.g. $E_{QZ}(x,y,z)$). This is done by transforming the cartesian coordinates to spherical coordinates (r,θ,φ) and running the TXF for each field evaluation point. Even though the process becomes more time consuming, the advantage of such a field reconstruction method is the lack of processing errors like the "end-point" issue typical of the conventional microwave holography (or planar back projection technique [1]).

III. Examples

Uncertainty budgets (UB) of SNF measurement systems are usually evaluated considering FF reconstruction distances. In this paper two different examples are considered to investigate the effect of measurements errors when arbitrary finite-distance field reconstructions are considered. The objective to derive some guidelines regarding the validity of available FF-based UB when a NF/NF transformation is considered in the process.

The following examples are reported in this section:

- SH400 dual-ridge horn measured in a Multi Probe Array (MPA) system
- Low Frequency PWG measured in a SNF system

A. *Dual-Ridge Horn (SH400)*

Measurements of the SH400 dual-ridge horn by MVG [12], working in the wide 400MHz to 6GHz frequency band, are considered. As depicted in Figure 2. the horn has been measured in a spherical MPA system tailored for automotive measurements. The horn fits into a 75cm-diameter minimum sphere while the measurement sphere diameter is 12m. The horn has been measured in the 0.4-4.0GHz band considering two different configurations:

- Onset configuration (centered horn, like in Figure 2.)
- Offset configuration (horn centered at x=1.5m, not shown in Figure 2.)

Although the MPA system has been optimized to minimize the measurement errors as much as possible, the following sources of uncertainty are expected to produce some differences in the radiation patterns measured in the two configurations:

- *Residual room scattering* (chamber reflections at lower frequencies)
- *Truncation errors* (truncation of scanning area at $\theta = 110°$, [13])
- *Probe pattern effect* (probe tapering effect at higher frequencies due to lack of probe compensation, [11])

As shown in Figure 2, several NF/NF transformations are computed considering reconstruction spheres with radii ranging from 50cm to 10m. According to the conventional formula ($2\,D^2/\lambda$, with D being the maximum AUT dimension and λ the wavelength), the FF distance of such horn is 1.5m at 400MHz and 15m at 4GHz. Reconstruction distances like 50cm, 100cm etc… are significantly smaller than the FF distance, hence interesting to investigate.

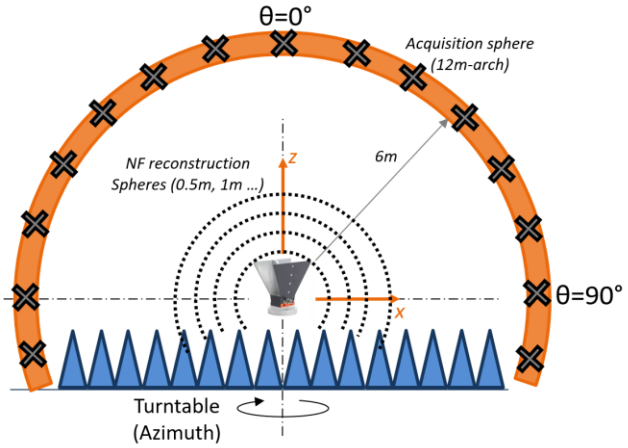

Figure 2. Illustration of the measurement scenario of the SH400 horn (onset configuration) and NF reconstruction spheres.

Figure 3. shows examples of gain normalized NF pattern reconstructions at 50cm and 100cm at the test frequencies of 1GHz (left) and 4GHz (right). The blue traces are obtained from the onset measurement of the SH400, while the red traces from the offset one. Of course, since we are comparing pattern at NF distance, the latter has been back-translated to the origin of the coordinate system in post-processing. For comparison, the FF patterns are also shown (bottom row of Figure 3.).

At 1GHz the agreement between the two measurements at the different reconstruction distances is good, however, some deviations at angles beyond +/-60° can be observed at two finite distances. At FF distance instead, the patterns correlation seems slightly better (up to +/-90°).

The deviations on the mean beam at 4GHz are most likely due to the tapering effect of the probe pattern which a such frequency deviates from a dipole-like antenna and affects the radiation patterns computed from the offset measurement of the AUT. Such an effect is visible at each reconstruction distance in an approximately equal manner.

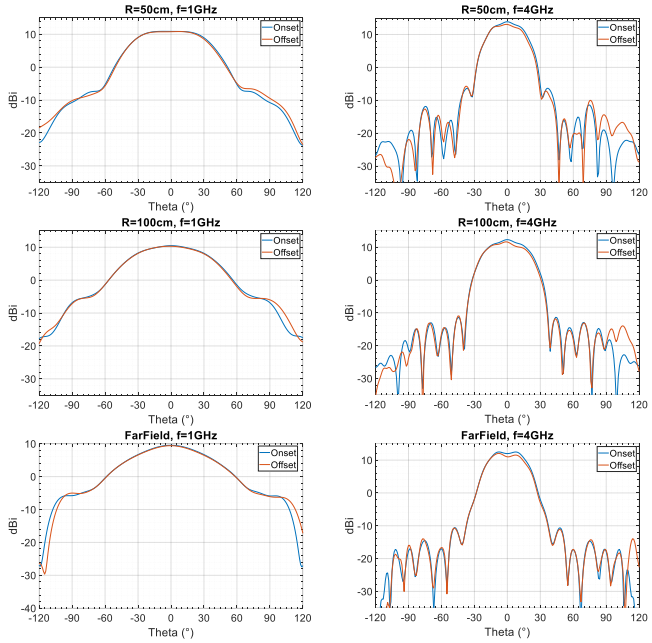

Figure 3. Examples of gain radiation pattern of the SH400 measured at two positions, evaluated at different reconstruction distances.

To better quantify the correlation between the patterns reconstructed at different distances, the Equivalent Noise Level (ENL) defined in equation (3) is considered. In such equation $E_i(\theta, \varphi)$ and $E_j(\theta, \varphi)$ are two radiation patterns to be compared (i.e. the patterns from the onset and offset measurement in this case) and RMS is the operator evaluating the Root Mean Square. In this analysis, the ENLs are evaluated up to $\theta = 90°$.

$$ENL = 20\log_{10}\left(RMS\left|\frac{E_i(\theta,\,\varphi) - E_j(\theta,\,\varphi)}{E_i(\theta,\,\varphi)_{MAX}}\right|\right) \qquad (3)$$

Figure 4. shows the ENL over frequency between the reconstructed patterns from the onset and offset measurements. The ENL quantifies the correlation between the two acquisitions, hence is an indicator of the measurement uncertainty. For this reason, is has been computed for each reconstruction distance, in order to observe any possible variations due to the different NF/NF transformation.

Due to the aforementioned probe pattern effect, which directivity increases with the frequency, the ENL increases beyond 2GHz. This expected trend is common to any reconstruction distance.

Below 2-2.5GHz, higher ENLs can be observed at shorter NF distances, namely 50, 100 and 150cm. Such electrically small reconstruction distances make the measurement errors more sensible resulting in more significant deviations between the two different acquisitions.

Even though more investigations are needed, this analysis suggests that when the radiated AUT field is reconstructed at electrically small distances, a re-assessment of the measurement uncertainty could be required.

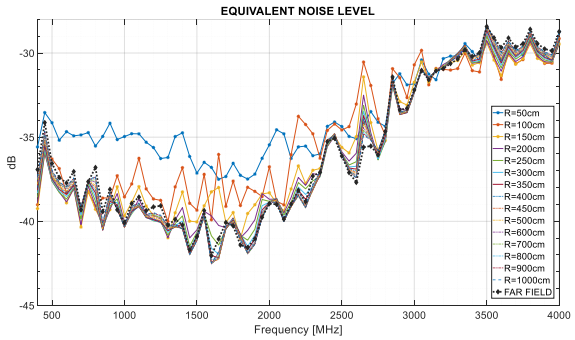

Figure 4. ENL between the two measurements of the SH400 at different positions, considering several field reconstruction distances in the data processing.

B. *Plane Wave Generator*

In this example, a low frequency PWG generator is considered [8]. A PWG is an array with suitable complex excitation of the antenna elements which creates a plane wave condition (i.e. field with flat amplitude and phase) in a NF region of the array, called Quiet Zone (QZ).

By changing the excitation coefficients, PWG systems like the considered one can operate over 10:1 bandwidth and more. For the sake of the generality, and scalability of the results, we describe such PWG in terms of the first nominal operating frequency, f_0, and its associated wavelength λ_0.

The considered PWG array dimension is $2\lambda_0$. With a proper setting of the excitation coefficients, the PWG system provides good QZ performances from f_0 to $10f_0$. In this analysis we consider a set of excitation coefficients synthesized for optimal QZ performances in the f_0-$2f_0$ frequency range. As depicted in Figure 5. the spherical QZ has a diameter of $1.3\lambda_0$ and is located at $3\lambda_0$ from the PWG.

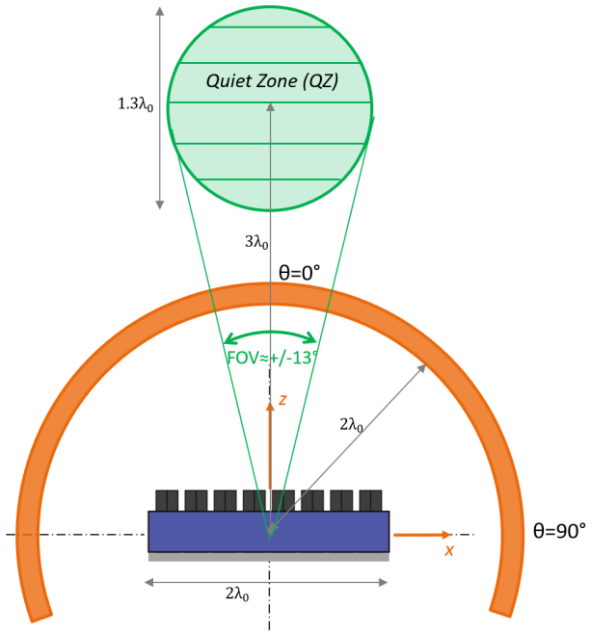

Figure 5. Illustration of the measurement scenario of the low frequency PWG in a SNF system with NF reconstruction in the QZ.

As also shown in Figure 5, such a PWG has been measured in a SNF range of measurement radius $2\lambda_0$. As described in section II, the NF/NF transformation process has been used in this case to compute the field in the QZ, in order to verify its field uniformity. Due to the electrically short scanning distance ($2\lambda_0$), the PWG has been measured at two different positions along the z-axis, in order to apply the λ/4-avering technique [14]-[15] and mitigate the effect of the multiple reflections. The considered array positions are:

- Onset (array at $z = 0$, position#1)
- Offset (array at $z = \lambda_0/4$, position#2)
-

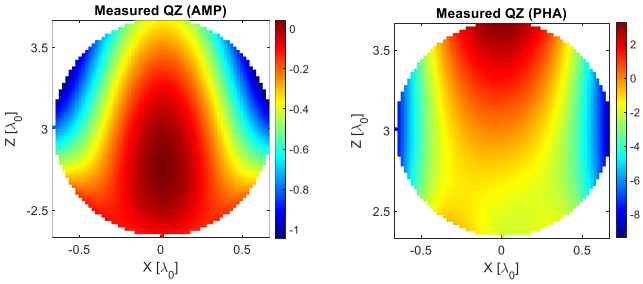

Figure 6. Example of QZ (downrange at y=0) obtained from SNF measurement of the PWG and NF/NF transformation at $1.5f_0$

An example of measured QZ at $1.5f_0$ is shown in Figure 6. Such amplitude and phase distributions have been obtained by first averaging the two datasets in the SWC domain, and then

computing the field in QZ with the TXF. The observed amplitude and phase uniformity is approx. +/-0.5dB and +/-5° respectively, is in line with the predicted results. The overall RMS QZ uniformity over frequency is shown in Figure 7. Such a metric is reported both considering the λ/4-average (green traces) and the individual measurements performed with the PWG in the two positions (blue and red traces). As expected, the λ/4-avering technique is able to reduce the uncertainty due to the measurement system.

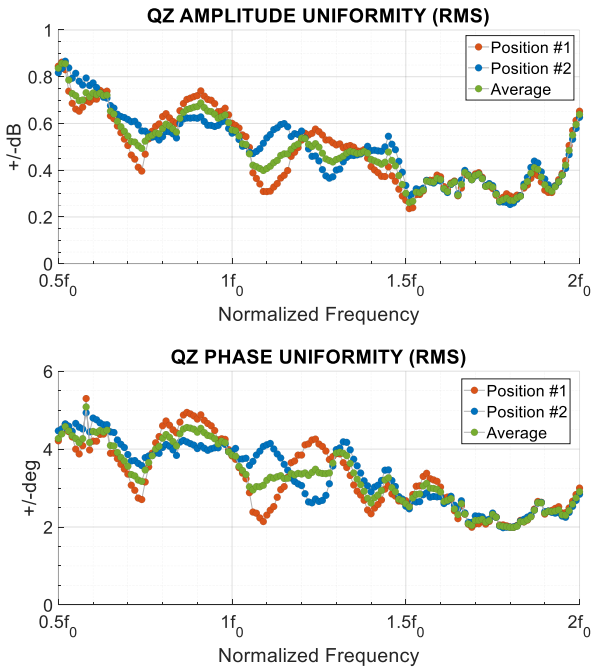

Figure 7. Amplitude (top) and phase (bottom) field uniformity in the QZ of the low frequency PWG.

The two measurement datasets are now exploited to investigate the "propagation" of the measurement errors when the NF/NF transformation is applied to evaluate the QZ performance instead of the more conventional NF/FF transformation process.

The FF pattern correlation between the two measurements of the PWG in different positions is again evaluated with the ENL metric reported in equation (3). Although the PWG is not designed to work at FF distance, the FF radiation patterns have been computed for both dataset in order to evaluate the "nominal" FF uncertainty. The ENL has been evaluated in the Field of View (FOV) of the QZ, illustrated in Figure 5 (+/-13°). The computed ENL is the blue trace shown in Figure 8.

The NF uncertainty resulting from the SNF acquisition, and the NF/NF transformation process has been evaluated from the point-wise ratio of the two QZ maps computed from the two PWG acquisition ($E_{QZ\#1}(x,y,z)$ and $E_{QZ\#2}(x,y,z)$), as depicted in equation (4). The computed equivalent interfering signal is reported in Figure 8 (red trace).

$$Interf = 20\log_{10}\left(RMS\left(\frac{E_{QZ\#1}(x,y,z)}{E_{QZ\#2}(x,y,z)}\right)-1\right) \qquad (4)$$

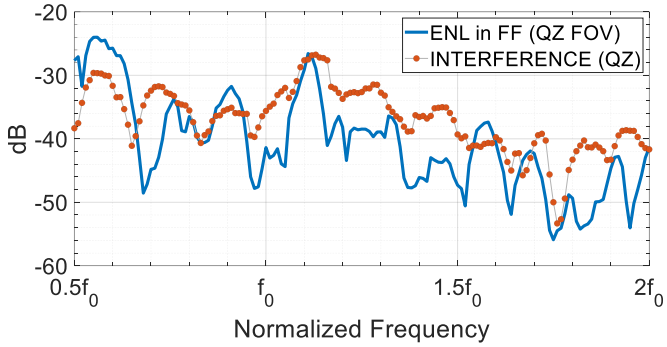

Figure 8. Comparison of uncertainty evaluted in FF versus uncertanty of the QZ reconstruction maps.

The agreement between the FF ENL, indicating the conventional FF uncertainty and the equivalent interfering signal obtained from the two computed QZs maps, indicating the NF uncertainty, are quite in line with each other. This suggests that uncertainty budgets of SNF ranges, determined assuming the conventional NF/FF transformation, can potentially be applied to the ranges when the NF/NF transformation is exploited to test the QZ of PWG, or similar antenna systems meant to operate at NF distance.

IV. Conclusions

The versatility of spherical near field systems allows effective tests of a large variety of device under tests, working either at conventional far field distances, or in specific near field regions, such as plane wave generators. While uncertainty budgets for typical FF figure of merits are usually readily available, the uncertainties of specific near field metrics are not.

In this paper we investigated the "propagation" of typical SNF measurement error sources when NF/NF transformations are performed instead of NF/FF. The considered experimental analysis include the SNF measurements of a dual-ridge horn and a PWG. In both cases, the uncertainties at the finite reconstruction distances are evaluated and compared to the FF uncertainty.

With the horn it has been observed that at significantly short field reconstruction distances, some measurement errors could become more sensible, hence a dedicated assessment of the uncertainty could be needed.

The uncertainty of the measured QZ of the PWG has been evaluated considering two different acquisitions of the device in the SNF range. The comparison with the corresponding FF uncertainty showed a similar trend and levels, suggesting that when the QZ performance of such devices are tested in SNF ranges, the available FF-based uncertainty budgets could be applied, avoiding time-consuming error analysis, tailored for a specific device under test.

REFERENCES

[1] IEEE Std 1720-2012 “Recommended Practice for Near-Field Antenna Measurements”

[2] J. E. Hansen (ed.), Spherical Near-Field Antenna Measurements, Peter Peregrinus Ltd., on behalf of IEE, London, United Kingdom, 1988

[3] O. Breinbjerg, "Spherical near-field antenna measurements — The most accurate antenna measurement technique," *2016 IEEE International Symposium on Antennas and Propagation (APSURSI)*, Fajardo, PR, USA, 2016, pp. 1019-1020, doi: 10.1109/APS.2016.7696217.

[4] F. Saccardi, A. Giacomini, L. J. Foged “Accurate Evaluation of Antenna Measurement Range Performance with the SWE Transmission Formula” AMTA 2023, October 8-13, Seattle, WA, USA

[5] IEEE Std 145™-2013, Standard for Definitions of Terms for Antennas

[6] 6G Wireless Communications: From Far-field Beam Steering to Near-field Beam Focusing

[7] F. Scattone, D. Sekuljica, A. Giacomini, F. Saccardi, A. Scannavini, E. Kaverine, S. Anwar , N. Gross, P. O Iversen, L. J. Foged “Preliminary Assesment of Millimeter Wave Plane Wave Generator For 5G Device Testing”EuCAP 2021, 22-26 March 2021, Düsseldorf, Germany

[8] V. Schirosi, F. Saccardi, A. Giacomini, F. Scattone, L. Scialacqua, A. Diamanti, E. Tartaglino, L.J. Foged, N. Gross, S. Anwar, E. Kaverine, P.O. Iversen, E. Szpindor “Accurate Antenna Characterisation at VHF/UHF Frequencies with Plane Wave Generator Systems”. AMTA 23, 7-13 October, Seattle, WA, USA

[9] S. Anwar, L. Scialacqua, A. Lelievre, M. Mantash, J. Luc, N. Gross, F. Saccardi, L.J. Foged, " Advanced Post-Processing Technique to Evaluate Specific Absorption Rate (SAR) for a Standard Dipole Antenna," *18th European Conference on Antennas and Propagation (EuCAP)*, Glasgow, 2024.

[10] F. Saccardi, A. Giacomini, L. J. Foged “Accurate Evaluation of Antenna Measurement Range Performance with the SWE Transmission Formula” AMTA 2023, October 8-13, Seattle, WA, USA

[11] F. Saccardi, A. Giacomini, L. J. Foged, T. Blin “Experimental Validation of Full Probe Correction Technique using Wideband and Dual-Polarized Probes in Spherical NF Antenna Measurements” AMTA 2021, October 24-29, Daytona Beach, FL, USA

[12] https://www.mvg-world.com/en/products/antennas/reference-antennas/dual-ridge-horns

[13] F. Saccardi, F. Rossi, L. Scialacqua, L. J. Foged, “Truncation Error Mitigation in Free-Space Automotive Partial Spherical Near Field Measurements”, AMTA 2017, 15-20 October, Atlanta, GA, USA

[14] L. J. Foged and others, ACE2 deliverable A1.2D2, “Recommendations and comparative investigations for near-field antenna measurement techniques and procedures”, Dec 2007

[15] R. T. Sánchez, F. Saccardi, A. Giacomini, M. A. Saporetti, P. Moseley and L. J. Foged, "Measurement of Low Frequency Antennas in Indoor Reflective Environments with the Synthetic Probe Array Technique" EuCAP *2022*, 27 March – 1 April, Madrid, Spain